



ISSN: 0067-2904

Role of Glycine-to-Nitrate Ratio in Physical and Magnetic Properties of Zn-Ferrite Powder

We'am Sami^{1*}, Zainab Sabeeh Sadeq²

¹Department of Physics, College of Education, University of Al-Qadisiyah, Qadisiyah, Iraq

²Department of Physics, College of Science, University of Baghdad, Baghdad, Iraq

Received: 24/4/2021

Accepted: 29/6/2021

Abstract

We report the influence of different glycine-to-nitrate ratios on the physical and magnetic properties for synthesized zinc-ferrite by microwave-assisted combustion route. Phase impurity and surface morphology investigated with XRD analysis and field emission-scanning electron microscopy, indicated that spinel structure were formed. Average particles size increased with the decrease of glycine to nitrate ratio. Magnetic measurement results indicated that high values of saturation magnetization were produced with low glycine/nitrate ratio. Optical properties of the investigated ferrites exhibited photo absorption from UV to visible region with energy gap values that decreased with the decrease of glycine-to-nitrate ratio. Mainly two broad metal-oxygen bands for zinc-ferrite were seen in FT-IR spectra.

Keyword: Glycine, Zn-ferrite, microwave-assisted, magnetic properties, spinel ferrite

دور نسبة الجلايسين - النترات في الخواص الفيزيائية والمغناطيسية لمسحوق فرايت الخارصين

وئام سامي^{1*} ، زينب صبيح صادق²

¹قسم الفيزياء، كلية التربية، جامعة القادسية، القادسية، العراق

²قسم الفيزياء، كلية العلوم، جامعة بغداد، بغداد، العراق

الخلاصة

تمت دراسة تأثير النسب المختلف للجلايسين إلى النترات ا على الخواص الفيزيائية والمغناطيسية لفرايت الزنك المصنعة باستخدام طريق الاحتراق بمساعدة الميكروويف. أظهرت نقاوة الطور وتشكلات السطح التي تم فحصها بتحليل XRD والمجهر الإلكتروني الماسح للانبعثات إلى تشكل بنية الإسبنيل بمتوسط حجم بلوري يزداد مع انخفاض نسبة الجلايسين إلى النترات. تبين نتائج القياسات المغناطيسية ان قيم مغنطة التشبع تمتلك قيمة عالية عندما تكون نسبة الجلايسين الى النترات اقل . أظهرت الخواص البصرية للفريتات التي تم فحصها امتصاصاً ضوئياً من الأشعة فوق البنفسجية إلى المنطقة المرئية مع انخفاض قيم فجوة الطاقة عند انخفاض نسبة الجلايسين إلى النترات. بين طيف FT-IR ان هناك نطاقتان عريضتان من الفلز - اوكسجين لفرايت الخارصين .

1.Introduction

Generally, ferrites are compounds of mixed oxides of iron and one or more other materials which have ferrimagnetic properties[1]. Based on their crystal structures, ferrites can be categorized into three groups: spinel, garnet, and hexagonal [2]. Ferrites are essential

*Email: weam.sami@qu.edu.iq

materials that are employed in the fabrication of magnetic, electronic and micro-wave devices[3]. Spinel-type ferrites of composition MFe_2O_4 [$M = Mn, Ni, Zn, Co, \text{etc.}$] exhibit interesting properties so that they have wide potential technological applications in different fields[4]. The nano zinc ferrite has been extensively studied among the spinel family by worldwide researchers due to their unique chemical and physical properties based on their size compared to the bulk counterpart materials[5]. When the particle size decreases, the volume fraction of atoms at surfaces or in interfaces increases. This gives rise to a modification of the thermal, electronic, optical, magnetic properties, etc., of nanostructured materials compared to their coarse-grained counterparts and strongly affects materials research in general [6]. Nano zinc ferrite is commonly used in magnetic resonance imaging, catalysis[7], sorbent material [8], biomedical fields and photocatalytic applications[7]. Recent studies have shown that the physical properties of nanoparticles are influenced by the process of their preparation. Since crystallite size, distribution of particle sizes, and interparticle spacing have the greatest impact on magnetism, so the ideal synthesis technique is the one that provides superior control over these parameters[9]. In recent years, Zinc ferrite particles have been prepared using different chemical and physical methods, such as co-precipitation [10], conventional heating (CHM) method [11], Solvothermal route [12], and sol-gel method [13] etc. However, most of the routes use complex processes, elevated reaction temperatures, long reaction times, toxic reagents, and advanced processing [14]. Microwave combustion route is gaining much interest among researchers, because of its features such as environment friendly route, rapid heating, high reaction rate, energy saving, and short reaction time [5]. Accordingly, the present work is aimed to synthesize zinc ferrite powders using microwave-assisted combustion route, using different glycine-to-nitrate ratio, and to examine their physical and magnetic properties.

2. Materials and Methods

Solutions of high purity nitrate salts of zinc and iron from HIMEDIA Co., India] were used with a molar ratio 1:2. Each was weighed separately in stoichiometric ratio and dissolved in a suitable quantity of de-ionized water. The solutions were mixed and stirred for 20 minutes. Amount of glycine from Central Drug House, India], with the chemical formula ($C_2H_5NO_2$), was added to the mixture with stirring. The mixture after 20 minutes was transferred to a microwave oven. The solution will boil, dehydrates and decomposes producing a lot of gases such as CO_2 , NO_2 , and N_2 . On reaching the combustion point, it will become solid. The resultant powder was washed 3 times with ethanol and distilled water and dried at ($70^\circ C$) for 2 hours. Finally, the powder was grounded for 2 minutes with a mortar to obtain fine powder. All these steps are shown in Figure 1. Three precursor solutions of different glycine-to-nitrate ratios (0.66, 0.5 and 0.33) were separately prepared by the above described procedure. The powders were analysed and characterized with XRD, FT-IR, EDAX, UV-Vis, and VSM.

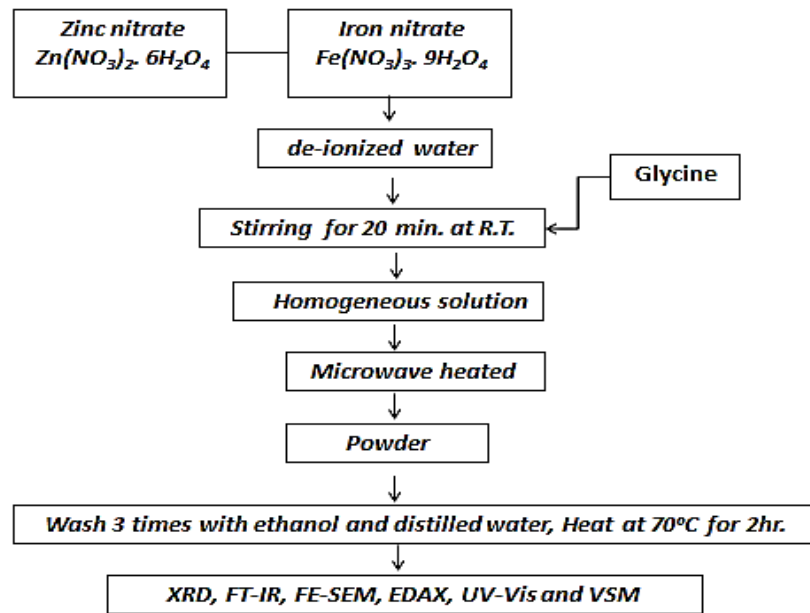


Figure 1- A schematic representation of microwave-assisted combustion route used for the synthesis of Zn-ferrite powder

3. Results and Discussion

3.1. Structure and Morphology Characterization

The XRD patterns [obtained using Shimadzu diffractometer model XRD 6000] of Zn-ferrite with various glycine-to-nitrate ratios are displayed in Figure 2. The peaks could be easily indexed as (220), (311), (222), (400), (422), (511), (440) and (533). All the planes are allowed planes, which indicates the formation of cubic spinel structure with a change in the lattice parameter from (8.44 to 8.39 Å) in accordance with the standard (JCPDS card No.22-1012) for zinc ferrite. Peak for impurity phase was observed in the Zn-ferrite XRD patterns (e.g. ZnO) for G/N ratio 0.66 and 0.50. This impurity phase decreased in the XRD pattern of the 0.33 G/N ratio, as shown in Figure 2. The G/N ratio decrease achieves an increment in grain size, leading to sharper and narrower peaks due to more crystalline peaks. This is noticed with the XRD pattern of Zn-ferrite of 0.33 G/N ratio showing sharper peaks than the previous peaks of the other two patterns, as shown in Table 1.

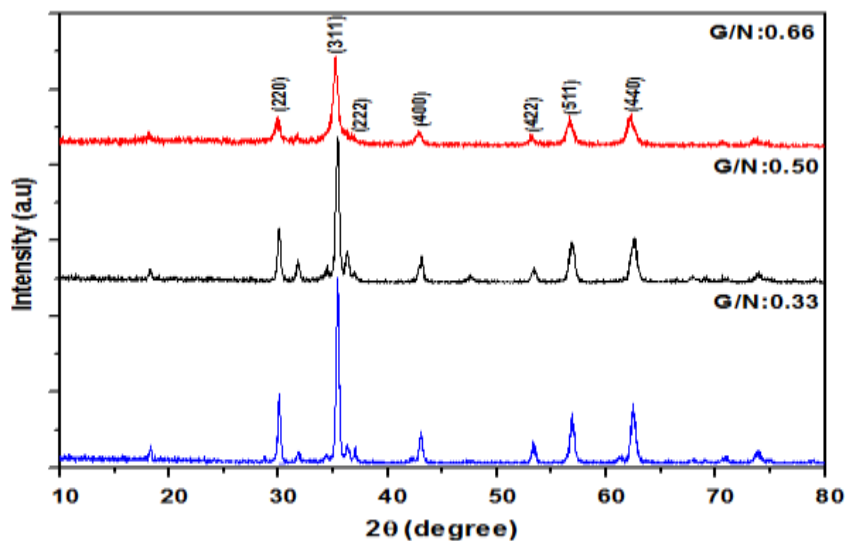


Figure 2-XRD patterns of Zn-ferrite powder at various glycine-to-nitrate ratios

The structure parameters, such as crystallite size (D) and lattice constant (a), of the highest peak at (311) plane in the XRD pattern for all samples were determined depending on Scherrer equation (Eq.1)[5] and Bragg law [14] and summarized in Table 1.

$$D = \frac{k\lambda}{\beta \cos\theta} \quad \dots\dots 1$$

$$a = d_{hkl} \sqrt{h^2 + k^2 + l^2} \quad \dots\dots 2$$

Where λ -represents XRD wavelength that was used (which was equal to 0.154 nm), β - is full width at half maximum of plane (311) , θ is the Bragg angle, d is the d-spacing value and (hkl) are the Miller indices.

Table 1-Structure parameters of Zn-ferrite powder at various glycine-to-nitrate ratio.

Samples	G/N ratio	FWHM β (deg.)	Lattice Constant a (Å)	Crystallite Size (XRD) D(nm)
S1	0.66	0.512	8.44	15.50
S2	0.50	0.378	8.40	23
S3	0.33	0.302	8.39	27.05

From Table 1, it is clear that a decrease in the glycine-to-nitrate ratio resulted in an increase of the crystallite size . Based on a previous research [15], crystallite size is related to the value of pH. When glycine-to-nitrate ratio is high, the value of the pH is high. There is a lot of gas emitted during the combustion process, in the microwave oven, leading to a decrease in crystallite size and an increase in porosity. This was also noted in our results as noticed from the FE-SEM images (Figure 3). Similar results were obtained by Lin et al. [15]. Literature have shown that lattice constant and crystallite size are directly related. Increasing in crystallite size leads to decrease or increase in the lattice constant. In the present work, decrease in the glycine-to-nitrate ratio [increase in particle size], have resulted in decrease of the lattice constant. Similar observes were obtained by T. Anjaneyulu et al. [16]. These results show that a change in the amount of fuel used in the synthesis leads to major changes in the powder structure.

3.2. Morphological and Chemical Composition Analysis

In Figure 3 the FE-SEM images at different scale by [Tescan Mira3 France] for Zn-ferrite are given. From the images, it is clear that the agglomerated nanoparticles with voids have a sphere-like form. Agglomeration can be caused by magnetic interactions between these particles or by organic compounds exhibited in the samples[17, 18]. Agglomerates produced during the microwave irradiation process of the microwave combustion method are highly probable. The effects of the escaped gases during the combustion phase could be the formation of the voids in the powdered samples. Similar findings were also seen in other studies [19, 20, 21].

EDAX analysis for Zn-ferrite, shown in Figure 4, indicates that the basic compositions of the samples are Zn, Fe and O. Al impurity peak appears in EDAX pattern of Zn-ferrite powder with 0.33 G/N ratio due to the sample coating. It could be due to a number of reasons and factors:

(i) different thicknesses of the coating layer (aluminum) for the three samples preparation for electron microscopy . The samples with 0.66 and 0.50 glycine to nitrate ratios

may possess better control over the aluminum coating layer compared with the sample of 0.33 glycine to nitrate ratio .

(ii) The sample with 0.33 glycine to nitrate ratio was tested at a different time than the samples with 0.66 and 0.50 glycine to nitrate ratios.

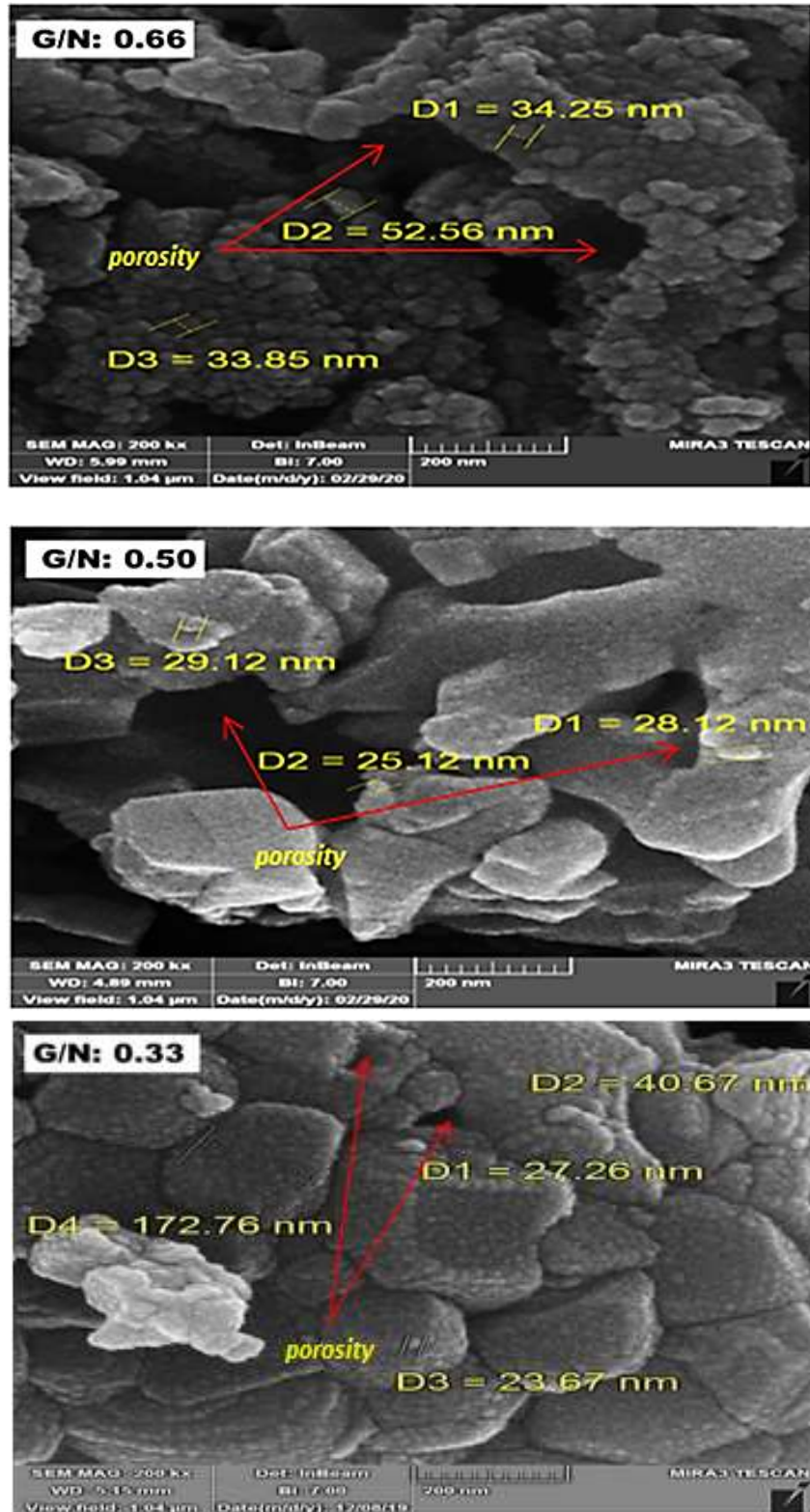


Figure 3- FE-SEM images of Zn-ferrite powder at various glycine-to-nitrate ratios

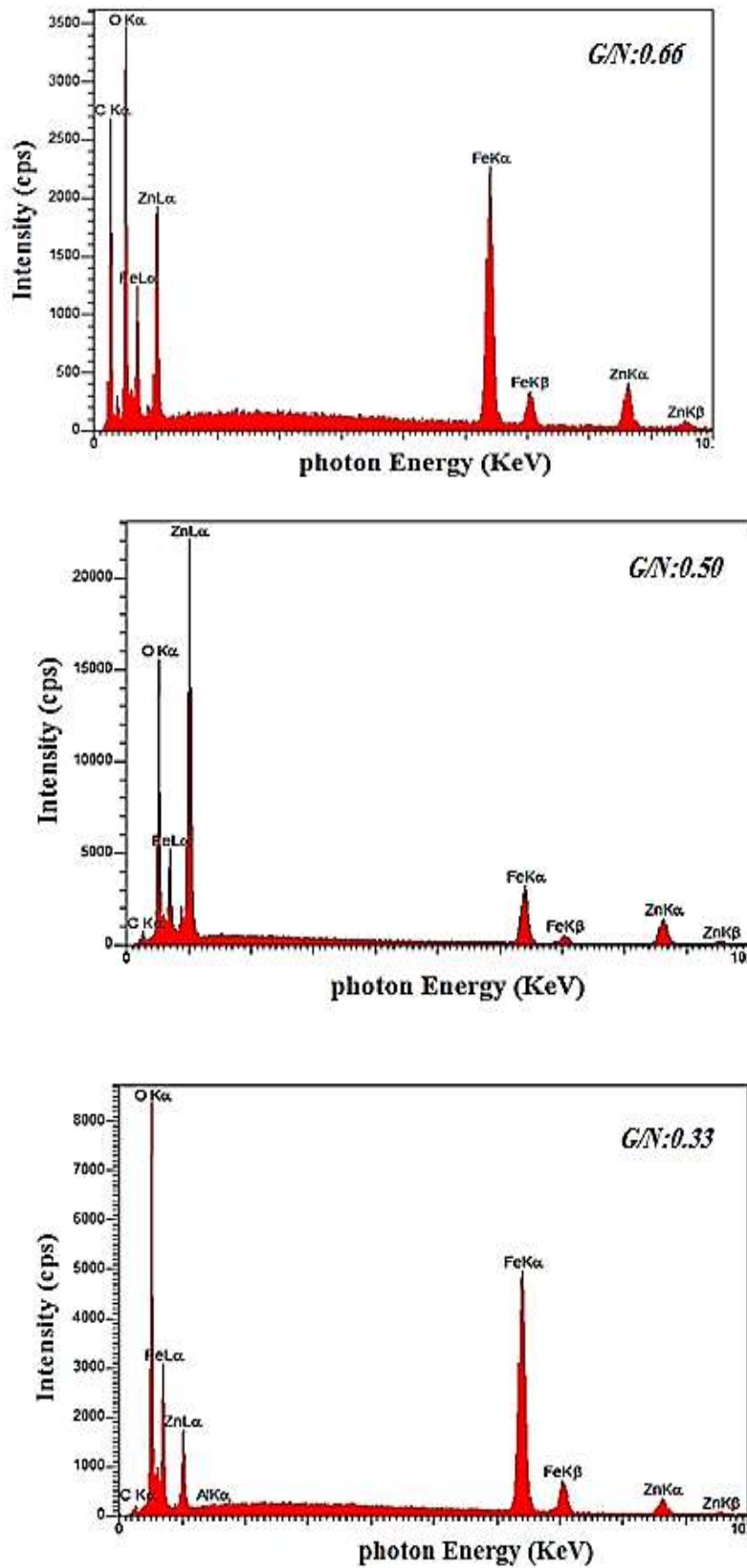


Figure 4-EDAX analysis of Zn-ferrite powder at various glycine-to-nitrate ratios

3.3 Fourier Transforms - Infrared Spectroscopy Characterization

The FTIR spectra of Zn-ferrite was recorded with a spectrometer (Shimadzu-8400S) at the wavelength range ($4000 - 450 \text{ cm}^{-1}$) is depicted in Figure 5.

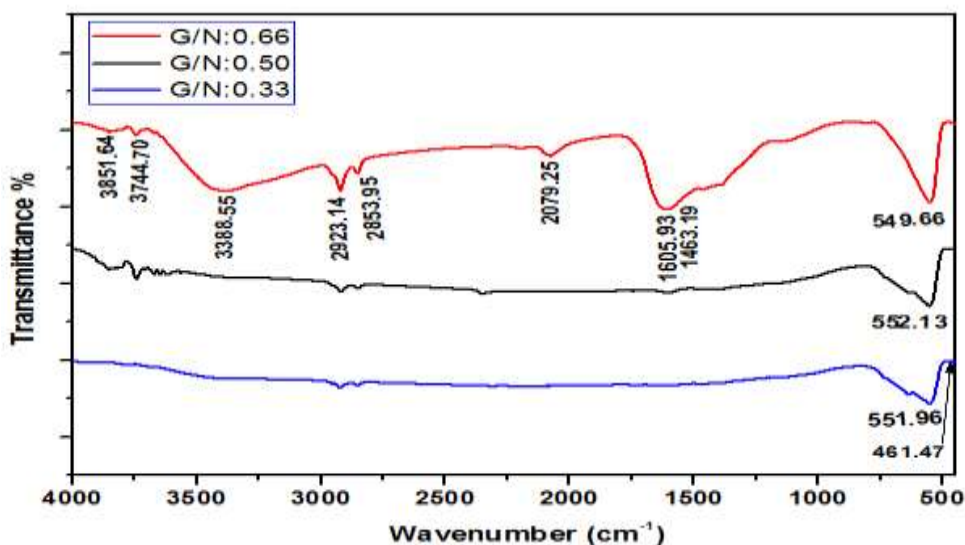


Figure 5- FT-IR spectra of Zn-ferrite powder at various glycine-to-nitrate ratios

Broad metal-oxygen bands were seen in all samples, ferrites bands, in particular, were typically observed in the range $600-500 \text{ cm}^{-1}$. It is clear that no new bands appeared around the range of 600 cm^{-1} . However, two peaks at 551.96 and 461.47 cm^{-1} appeared in the spectrum for the sample S3 at G/N: 0.33 indicating the formation of spinel ferrite structure. The afore mentioned two peaks also confirmed the formation of tetrahedral and octahedral structures. Similar results were observed in other studies [22, 23].

3.4. UV - Visible Analysis

The absorption of Zn-ferrite of different ratios of G/N as a function of wavelength were obtained with Shimadzu spectrophotometer [UV1800] as shown in Figure 6. Zn-ferrite demonstrated extended photo absorption from UV to the visible region. This is very compatible with the results of Suppuraj et al. [24].

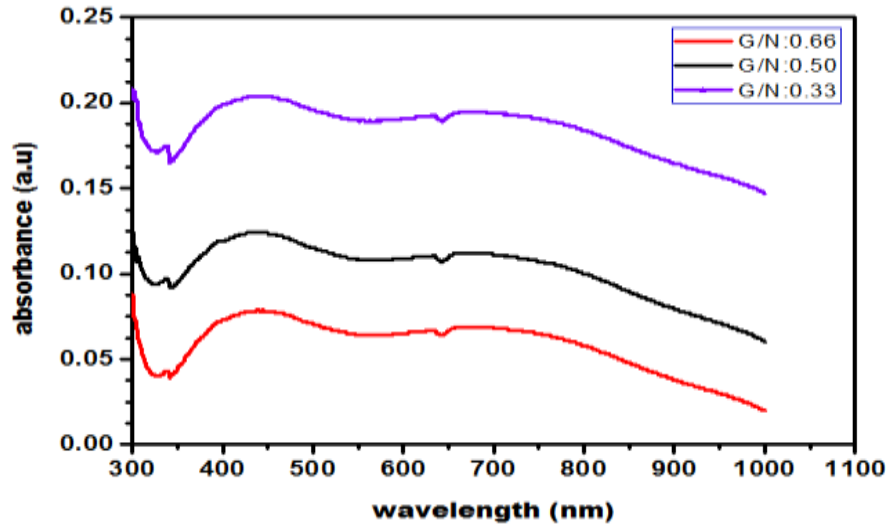


Figure 6-Absorption as a function of wavelength of the Zn-ferrite at various glycine-to-nitrate ratios In order to estimate the optical band gap for samples, Tauc-relation is commonly used. The derivation of the band gap energy from the plots $(\alpha h\nu)^2$ as function of the incident energy ($h\nu$) is shown in Figure 7. The optical gap is defined as occurring through solid lines at the intercept of the linear extrapolation to the Y axis.

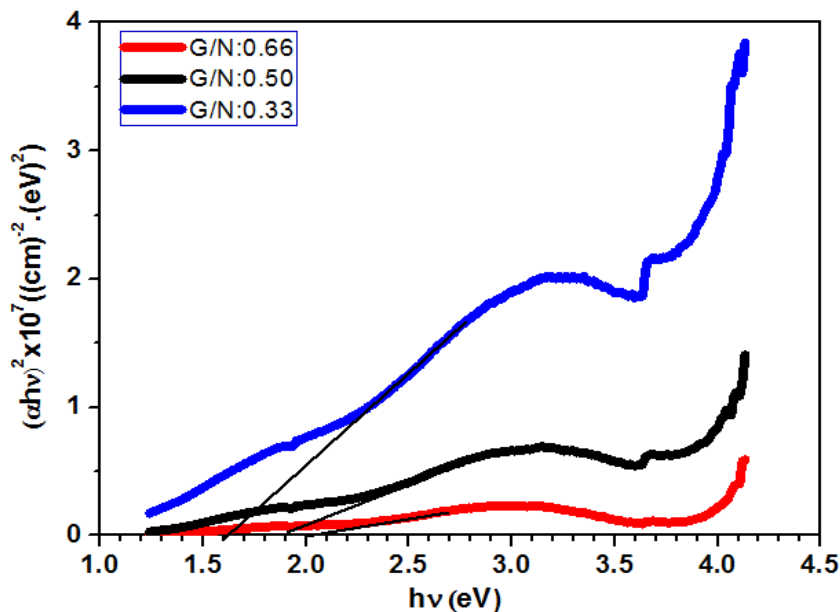


Figure 7-Plot of $(\alpha h\nu)^2$ versus $h\nu$ of Zn-ferrite powder at various glycine-to-nitrate ratios

In general, various parameters can affect and cause an increase in the optical band gap, such as crystallite size, impurities, and lattice strain [17]. In this work, the decrease in the optical band gap with the decrease of glycine-to-nitrate ratio [increase in particle size] was clearly seen. The obtained data revealed that the optical band gap for Zn-ferrite decreased from (2 to 1.6) eV as G/N was increased from 0.66 to 0.33. These energy gap values are in very good accordance with earlier reported values [24] [25]. Zn-ferrite band gap energy has been recorded at (2.3, 2.0, 1.9, 1.7 and 1.6) eV by many researchers [25].

3.5. Magnetic Measurements

Zn-ferrite exhibited typical magnetic behavior. The hysteresis loops of Zn-ferrite (as recorded by VSM, MDK, performed in Iran) are shown in Figure 8.

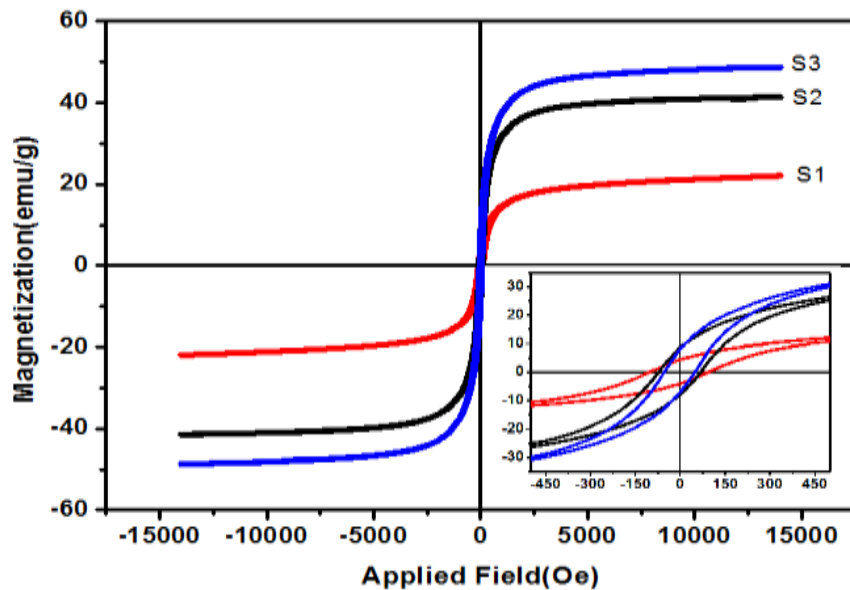


Figure 8-Magnetic hysteresis loops of Zn-ferrite powder at various glycine-to-nitrate ratios, (S1) G/N: 0.66, (S2) G/N: 0.50, (S3) G/N: 0.33 [coercivity Hc plot insert]

From Figure 8, it is clear that the remanence and saturation magnetization values increased by decreasing glycine-to-nitrate ratio (bigger particles size). One of the important reasons for this enhancement is the migration of Fe^{+3} into tetrahedral site, which eventually restructure the magnetic interaction between the octahedral and tetrahedral crystalline positions. The values of magnetic parameters such as remanence magnetization (Mr), saturation magnetization (Ms) and coercivity (Hc) of the ferrites have been directly extracted from these curves and listed in Table 2.

Table -2 Magnetic measurements extracted from hysteresis loops of Zn-ferrite at various glycine-to-nitrate ratio.

Samples	G/N ratio	Ms (emu/g)	Mr (emu/g)	Hc (Oe)	Mr/Ms
S1	0.66	22.12	5	90	0.22
S2	0.50	41.37	9	70	0.21
S3	0.33	48.75	8	50	0.16

From Table 2, it is clear that as the glycine-to-nitrate ratio increased, the coercivity value was decreased. The coercivity for these samples were found to decrease from (90 to 50) Oe as glycine-to-nitrate ratio decreased from 0.66 to 0.33. Generally, as the particle size increases [within the single domain region] coercivity increases. In order to explain the effect of reducing domain, squareness ratio was calculated for each sample. A squareness ratio of about 0.5 means that a single magnetic domain sample has been produced [26]. From Table 2, it is also clear that Zn-ferrite have single domain structures. Magnetic properties of ferrites also relies on the preparation route [16]. Different values of the saturation magnetization for Zn-ferrite by different methods were reported such as (50.43), (82), (30), (12), (60) and 22.12-48.75emu/g [3, 27, 28].

4. Conclusion

Three samples of the spinel Zn-ferrites have been successfully synthesized by microwave combustion route. The results revealed : (i) This route via glycine provides a simple route, rapid and environmental friendly using cheap precursors and needs short time, (ii) The fuel amount has a major impact on structure , optical and magnetic properties. Spinel structure was formed with particle size that increased with the decrease of glycine – to -nitrate ratio. In our experiment the 0.33 glycine – to -nitrate ratio achieved an improvement in grain size and cubic spinel type lattice of $ZnFe_2O_4$ without trace of other impurity phase, (iii) Optical properties for the investigated ferrites exhibited photo absorption from UV to visible region . The energy gap decreased with the decrease of glycine-to-nitrate ratio, and (iv) High values of saturation magnetization was produced with low values of glycine – to - nitrate ratio.

References

- [1] T. S. Mahdi and F. J. Kadhim, "Effect Depositions Parameters on the Characteristics of $Ni_{0.5}Co_{0.5}Fe_2O_4$ Nanocomposite Films Prepared by DC Reactive Magnetron Co-Sputtering Technique", *Iraqi Journal of physics (IJP)*, vol.18, no.45, pp. 76-88, 2020. DOI: 10.20723/ijp.18.45.76-88.
- [2] S. S. Shinde, "Crystal Structure and Magnetic Interactions of Ferrites", *International Journal of Science and Research (IJSR)*, vol. 5, no. 11, pp. 1034-1036, 2016 . www.ijsr.net.
- [3] M. F. Al-Hilli, " Characteristics of AC. Conductivity and Dielectric Behavior of $Cu_{0.5}Ti_{0.5}HoxFe_{2-x}O_4$ Ferrites", *Iraqi Journal of Science*, vol. 57, no. 3C, pp. 2245 -2251, 2016.
- [4] M. Kooti and A. N. Sedeh, "Glycine-Assisted Fabrication of Zinc and Manganese Ferrite Nanoparticles", *Scintia Iranica F.*, vol. 19, no. 3, pp. 930 – 933, 2012. doi:10.1016 /j.scient.2012.02.020.
- [5] A. Manikandan, J. J. Vijaya, M. Sundararajan, C. Meganathan, L. J Kennedy, and M. Bououdina, "Optical and Magnetic Properties of Mg-doped $ZnFe_2O_4$ Nanoparticles Prepared by Rapid Microwave Combustion Method", *Superlattices and Microstructures*, vol. 64, pp. 118-131, 2013 . <http://dx.doi.org/10.1016/j.spmi.2013.09.021>.
- [6] H.-E. Schaefer, "*Nanoscience: The Science of the Small in Physics, Engineering, Chemistry, Biology and Medicine*". Springer, 2010, 3 . DOI 10.1007/978-3-642-10559-3
- [7] J. Mayekar, V. Dhar, and S. Radha, "Synthesis, Characterization and Magnetic Study of Zinc Ferrite Nanoparticles", *International Journal of Innovative Research in Science, Engineering and Technology*, vol. 5, no. 5 , pp. 8367-8371, 2016. DOI:10.15680/IJIRSET.2016.0505268.
- [8] I. A. Amar, S. I. Faraj, M. A. Abdulqadir, I. A. Abdalsamed, F. A. Altohami, and M. A. Samba, "Oil Spill Removal from Water Surfaces Using Zinc Ferrite Magnetic Nanoparticles As a Sorbent Material", *Iraqi Journal of Science*, vol. 62, no. 3, pp. 718 -728, 2021. DOI: 10.24996/ijis.2021.62.3.2.
- [9] C. T. Seip, E. E. Carpenter, C.s J. O'Connor, V.T. John and Sichu Li "Magnetic Properties of a Series of Ferrite Nanoparticles Synthesized in Reverse Micelles", *Ieee Transactions On Magnetics*, vol. 34, no. 4, pp. 1111-1113, 1998.
- [10] I. Ud Din, S. Tasleem, A. Naeem, M. S. Shaharun, and G. M. J. Al Kaisy, "Zinc Ferrite Nanoparticle Synthesis and Characterization; Effects of Annealing Temperature on the Size of Nanoparticles". *Australian Journal of Basic and Applied Sciences*, vol. 7, no. 4, pp. 154-162, 2013.
- [11] R. C. Sripriya, S.A. Ezhil, J. Madhavan, and M.A.R. Victor , "Synthesis and Characterization Studies of $ZnFe_2O_4$ Nanoparticles", *Mechanics, Materials Science & Engineering*, vol. 9, no. 1, pp. 13-17, 2017 . <https://hal.archives-ouvertes.fr/hal-01496352>.
- [12] C. G. Anchieta, A. Cancelier, M. A. Mazutti, S. L. Jahn, R. C. Kuhn, A. Gündel, O. Chiavone-Filho, and E. L. Foletto, "Effects of Solvent Diols on the Synthesis of $ZnFe_2O_4$ Particles and Their Use As Heterogeneous Photo-Fenton Catalysts", *Materials*, vol. 7, no. 9, pp. 6281-6290, 2014 .

Doi:10.3390/ma7096281.

- [13] M.G. Naseri, E. B. Saion, and A.H. Shaari, "Role of PVP on the Phase Composition and Morphology of Manganese Ferrite Nanoparticles Prepared by Thermal Treatment Method", in Proceedings of the 2nd International Conference on Environment Science and Biotechnology, IPCBEE vol.48,2012 .
- [14] M. Venkatesh, G. S. Kumar, S. Viji, K.Sekar, and E.K. Girija, "Microwave Assisted Combustion Synthesis and Characterization of Nickel Ferrite Nanoplatelets", *Modern Electronic Materials*, vol. 2, no. 3, pp. 74-78, 2016 .
<https://doi.org/10.1016/j.moem.2016.10.003>.
- [15] Q. Lin, J. Xu, F. Yang, J. Lin, H. Yang, and Y. He, "Magnetic and Mössbauer Spectroscopy Studies of Zinc-Substituted Cobalt Ferrites Prepared by the Sol-Gel Method", *Materials*, vol. 11, no. 10, p. 1799, 2018.
Doi:10.3390/ma11101799.
- [16] T. Anjaneyulu, A. Raghavender, K. V. Kumar, P. N. Murthy, and K. Narendra, "Effect of Particle Size on the Structural and Magnetic Properties of Nanocrystalline Zinc Ferrite", *Sci. Technol. Arts Res. J.*, vol. 3, no. 3, pp. 48-51, 2014.
DOI: 10.4314/star.v3i3.8.
- [17] A. T. Dhiwahara, M. Sundararajan, P.Sakthivel, C. S. Dashd, and S. Yuvaraj. "Microwave-Assisted Combustion Synthesis of Pure and Zinc-Doped Copper Ferrite Nanoparticles: Structural, Morphological, Optical, Vibrational, and Magnetic Behavior", *Journal of Physics and Chemistry of Solids*, vol. 138, p. 109257 (36P), 2020 .
Doi.org/10.1016/j.jpms.2019.109257.
- [18] P. Tehranian, A. Shokuhfar, and H. Bakhshi, "Tuning the Magnetic Properties of ZnFe₂O₄ Nanoparticles Through Partial Doping and Annealing", *Journal of Superconductivity and Novel Magnetism*, vol. 32, pp. 1013-1025, 2018.
Doi.org/10.1007/s10948-018-4785-6.
- [19] P. Jadhav, K.Patankar, V.Mathe, N.L.Tarwal, J-H. Jang, and V. Puri, " Structural and Magnetic Properties of Ni_{0.8}Co_{0.2}-2xCu_xMnxFe₂O₄ Spinel Ferrites Prepared via Solution Combustion Route", *Journal of Magnetism and Magnetic Material*, vol. 385, pp. 160–165, 2015.
www.elsevier.com/locate/jmmm.
- [20] H. Masoudi, R. Sepahvand, E. Khosravi, and B. Nayebi, "Structural and Magnetic Properties of Co_{1-x}MgxFe₂O₄ Nanoparticles Synthesized by Microwave-Assisted Combustion Method", *J Supercond Nov Magn.*, vol. 30, no. 7, pp. 1801-1805, 2017.
DOI 10.1007/s10948-017-3974-z.
- [21] B. Hangai, E. Borsari, E. C. Aguiar, F. G. Garcia, E. Longo, and A. Z. Simões," Superparamagnetic Behaviour of Zinc Ferrite Obtained by the Microwave Assisted Method", *J Mater Sci: Mater Electron.*, vol. 28, pp. 10772-10779, 2017.
DOI 10.1007/s10854-017-6854-1.
- [22] T. M. Hammad, J. K. Salem, A. A. Amsha, and N K. Hejazy, "Optical and Magnetic Characterizations of Zinc Substituted Copper Ferrite Synthesized by a Co-Precipitation Chemical Method", *Journal of Alloys and Compounds*, vol. 741, pp. 123-130, 2018.
<https://doi.org/10.1016/j.jallcom.2018.01.123>.
- [23] M. Shahid, L. Jingling, Z. Ali, I. Shakir, M. F. Warsi, R.Parveen, and M. Nadeem, "Photocatalytic Degradation of Methylene Blue on Magnetically Separable MgFe₂O₄ Under Visible Light Irradiation", *Materials Chemistry and Physics*, vol. 139, no. 2-3, pp. 566-571, 2013.
<http://dx.doi.org/10.1016/j.matchemphys.2013.01.058>
- [24] P. Suppuraj, G. Thirunarayanan, M. Swaminathan, and M. Inbasekaran, "Facile Synthesis of Spinel Nanocrystalline ZnFe₂O₄: Enhanced Photocatalytic and Microbial Applications", *Materials Science and Applied Chemistry*, vol. 34, no. 1, pp. 5-11, 2017.
DOI: 10.1515/msac-2017-0001.
- [25] M. Movahedi, F. Kazemi-Cheryani, N. Rasouli, and H. Salavati, " ZnFe₂O₄ Nanoparticle: Synthesis and Photocatalytic Activity Under UV-Vis and Visible light", *Iran. Chem. Commun.*, vol. 3, pp. 137-142, 2015.
<https://www.researchgate.net/publication/281462033>.

- [26] V. Badwaik, D. Badwaik, V. Nanoti, and K. Rewatkar, " Study of Some Structural and Magnetic Properties of $\text{Sr}_2\text{Me}_2\text{Fe}_{11}(\text{SnCo})_{0.5}\text{O}_{22}$ Nano Ferrites", *International Journal of Knowledge Engineering*, vol. 3, no. 1, pp. 58-60, 2012.
<http://www.bioinfo.in/contents.php?id=40>.
- [27] Md. Amir, H. Gungunes, A. Baykal, M. A. Almessiere, H. sōzeri, I. Ercan, M. Sertkol, S. Asiri, and A. Manikandan, " Effect of Annealing Temperature on Magnetic and Mössbauer Properties of ZnFe_2O_4 Nanoparticles by Sol-Gel Approach", *Journal of Superconductivity and Novel Magnetism*, vol. 31, , pp. 3347–3356, 2018.
DOI: 10.1007/s10948-018-4610-2.
- [28] N. M. Deraz and A. Alarifi, "Microstructure and Magnetic Studies of Zinc Ferrite Nanoparticles", *International Journal of Electrochemical Science*, vol. 7, no.7, pp. 6501–6511, 2012.
www.electrochemsci.org